

OPEN ACCESS

EDITED BY

Yong-Jun Chen,
Southwest University, China

REVIEWED BY

Ye Yuan,
Shantou University, China
Shuai Chen,
Wuhan University, China

*CORRESPONDENCE

Huifan Liu
✉ lm_zkng@163.com

SPECIALTY SECTION

This article was submitted to
Aquatic Physiology,
a section of the journal
Frontiers in Marine Science

RECEIVED 26 November 2022

ACCEPTED 06 February 2023

PUBLISHED 21 February 2023

CITATION

Zou C, Fang Y, Lin N, Xiao G, Lin L
and Liu H (2023) Polysaccharide
extracted from pomelo fruitlets attenuate
hepatic lipid accumulation in hybrid
groupers (*Epinephelus lanceolatus* ♂ ×
Epinephelus fuscoguttatus ♀).
Front. Mar. Sci. 10:1108608.
doi: 10.3389/fmars.2023.1108608

COPYRIGHT

© 2023 Zou, Fang, Lin, Xiao, Lin and Liu. This
is an open-access article distributed under
the terms of the [Creative Commons
Attribution License \(CC BY\)](https://creativecommons.org/licenses/by/4.0/). The use,
distribution or reproduction in other
forums is permitted, provided the original
author(s) and the copyright owner(s) are
credited and that the original publication in
this journal is cited, in accordance with
accepted academic practice. No use,
distribution or reproduction is permitted
which does not comply with these terms.

Polysaccharide extracted from pomelo fruitlets attenuate hepatic lipid accumulation in hybrid groupers (*Epinephelus lanceolatus* ♂ × *Epinephelus fuscoguttatus* ♀)

Cuiyun Zou¹, Yuke Fang², Nuoyi Lin², Gengsheng Xiao³,
Li Lin¹ and Huifan Liu^{2*}

¹Guangdong Provincial Water Environment and Aquatic Products Security Engineering Technology Research Center, Guangzhou Key Laboratory of Aquatic Animal Diseases and Waterfowl Breeding, Zhongkai University of Agriculture and Engineering, Guangzhou, Guangdong, China, ²College of Light Industry and Food, Zhongkai University of Agriculture and Engineering, Guangzhou, Guangdong, China, ³Sericultural & Agri-Food Research Institute Guangdong Academy of Agricultural Sciences/Key Laboratory of Functional Foods, Ministry of Agriculture/Guangdong Key Laboratory of Agricultural Products Processing, Guangzhou, China

Introduction: Pomelo is one of the most consumed fruits due to its distinct flavor and sour taste, while large quantities of pomelo fruitlets discard during cultivation and most of them are disposed of as wastes. Such an issue has led to some research on how to make a high value-added reutilization of these fruitlets. Therefore, it was aimed to determine the structural characteristics of the polysaccharide of pomelo fruitlets and evaluate its attenuating effect on the hepatic lipid accumulation in hybrid groupers (*Epinephelus lanceolatus* ♂ × *Epinephelus fuscoguttatus* ♀).

Methods and results: In this research, YZ-0.5A is a 15,332 Da NaCl-soluble polysaccharide extracted from pomelo fruitlet which was characterized to mainly contain galactose and galacturonic acid and its putative structure was proven to be →2,4)- α-L-Rhap-(1→4)-α-D-GalAp-(1→4)-α-D-GalAp-(1→ with 3 branches. *In vivo* study, five isolipidic diets (containing 15% lipid) were fed to the groupers with an initial weight of 13.46 ± 0.08 g for 8 weeks, of which the dietary level of YZ-0.5A was 0 mg/kg (control), 150 mg/kg, 300 mg/kg, 600 mg/kg and 1200 mg/kg respectively. We found that the treatment of YZ-0.5A, especially 600 mg/kg, exerted an improved effect on the excessive lipid accumulation in grouper fed with a high-fat diet. *In vitro*, three graded concentrations of YZ-0.5A (75, 150 or 300 μg/ml) were added to the grouper primary hepatocytes respectively after incubation with 20% lipid emulsion (2 ml/L). The signs of recovery on morphological features observed under examined by histological evaluation supported the lipid lowering effect of YZ0.5-A. Further investigation showed that YZ0.5-A mitigated lipid emulsion-induced irregular lipid deposition

by regulating various lipometabolism-related indicators, thereby alleviating oxidative stress and apoptosis.

Discussion: Overall results exhibited the therapeutic potential of YZ0.5-A and elucidated its underlying mechanism in the fish with excessive lipid deposition, which first suggested the feasibility of reprocessing discarded pomelo fruitlet as medicine in aquaculture.

KEYWORDS

pomelo fruitlet polysaccharide, structural characterization, hybrid grouper, lipid emulsion, high fat diet

1 Introduction

Excessive fat is currently served as a partial protein substitute to optimize aquafeed costs in intensive aquaculture (Dai et al., 2019). Although a certain range of dietary lipids reportedly has an improved effect on a fish's growth performance (Zou et al., 2019), excessive lipid intake can inversely result in unwanted lipid deposition in fish (particularly in the liver) and augment vulnerability to an irregular metabolism, as previously reported in grass carp (*Ctenopharyngodon idella*) (Jia et al., 2020) and tilapia (*Oreochromis niloticus*) (Cao et al., 2019). High lipid accumulation in the liver is considered to be the leading contributor to fatty liver disease in farmed fish, which induces several metabolic disorders, including oxidative stress, inflammation, lipotoxicity, and apoptosis (Yu et al., 2021). The occurrence of fatty liver disease in fish is ever-increasing year by year, seriously threatening the sustainable development of the aquaculture industry.

Polysaccharides, due to their manifold pharmacological functions and reduced side effects, have been increasingly adopted in many fields, including the food, chemical, and pharmaceutical industries (Benhura and Chidewe, 2002). Recently, a growing body of literature has shown the pharmacological effect of polysaccharides, particularly extracted from plants, in diseases inflicted by abnormal lipid metabolism, such as fatty liver disease (Wang et al., 2016) and diabetes (Khursheed et al., 2020), which suggests its potential fat lowering effect. The polysaccharides added to the aquafeed are generally used as feed additives or functional supplements to promote growth performance, enhance immunity response, and ameliorate antioxidant status (Liu et al., 2021; Yu

et al., 2022). However, the discussion over whether polysaccharides have a positive effect on fish suffering from diet-induced lipid metabolic disorders is still ongoing.

Pomelo (*Citrus grandis* Osbeck) is a citrus fruit grown in South China that produces a mass of discarded and unmarketable fruitlets because of physiological fruit drop or artificial fruit thinning during cultivation. These fruitlets discarded in the orchard not only cause considerable financial losses to farmers but also result in environmental pollution due to their easy fermentability. Hence, inventing new and profitable ways to reuse these fruitlets is necessary and meaningful. Noticeably, the pomelo's counterparts in the citrus class have shown a positive effect on lipid metabolism. For example, dietary hesperetin improves hepatic triglyceride accumulation in rats fed orotic acid (Cha et al., 2001). Moreover, Zang et al. (2014) found that the peel of Yuzu (*Citrus junos* Siebold ex Tanaka) ameliorates diet-induced obesity in zebrafish (*Danio rerio*). Considering the reported bioactive effects on lipid metabolism of polysaccharides and citrus fruit, we hypothesized that the polysaccharide derivative from pomelo fruitlets may be reutilized as an aquafeed additive to normalize the diet-induced lipid metabolic disturbance.

The hybrid grouper (*Epinephelus lanceolatus* ♂ × *Epinephelus fuscoguttatus* ♀) has been largely farmed in southeastern coastal areas of China with the advantages of fast growth rate, strong resistance, and high economic and nutritious value (Liang et al., 2020). In the present study, we investigated the structure of the polysaccharide YZ0.5-A extracted from pomelo fruitlets and evaluated the effects of YZ0.5-A on lipid accumulation in the hybrid groupers *in vivo* and *in vitro*.

2 Materials and methods

2.1 Chemicals and reagents

Pomelo fruitlets cultivated in the Guangdong Province, China, were purchased from Meizhou Market (Meizhou, China). Cellulase, pectinase, and monosaccharide standards (analytical grade) were purchased from Shanghai Yuanye Bio-Technology Co., Ltd (Shanghai, China). Trifluoroacetic acid was purchased from

Abbreviations: ACO1, Aconitase 1; AMPK, AMP-activated protein kinase; CAT, catalase; condition factor (K); FAS, fatty acid synthase; FE, feed efficiency; FBW, final body weight; FT-IR, Fourier transform infrared spectroscopy; GSH-Px, glutathione peroxidase; GR, glutathione reductase; G6PD, glucose-6-phosphate dehydrogenase; H&E, hematoxylin & eosin; HSI, hepatosomatic index; HFD, high-fat diet; HPGPC, high-performance gel-permeation chromatography; HPAEC, high-performance anion exchange chromatography; LE, lipid emulsion; ME1, malic enzyme 1; PBS, phosphate-buffered saline; SOD, superoxide dismutase; VSI, viscerosomatic index; WG, weight gain.

Sinopharm Chemical Reagent (Shanghai, China). DEAE-Sepharose Fast Flow and Sephadex G-200 were purchased from Sigma-Aldrich (St. Louis, MO, USA). MEM culture medium was purchased from Thermo Fisher Scientific (SUZHOU) Instruments Co., Ltd. phosphate buffered saline (PBS) was purchased from Yongjin Biotechnology Co., Ltd. (Guangzhou, China). CCK-8 assay kits were purchased from the Biyuntian Institute of Biotechnology (Shanghai, China). The ELISA Kits for the determination of Superoxide dismutase (SOD), catalase (CAT), glutathione peroxidase (GSH-Px), and glutathione reductase (GR) were purchased from the Beyotime Institute of Biotech (Shanghai, China). lipid emulsion (LE) was purchased from Guangzhou Panyu Armed Police Hospital (Guangzhou, China). All other reagents and chemicals used in this study were of analytical grade.

The juvenile hybrid groupers (*Epinephelus lanceolatus*♂ × *Epinephelus fuscoguttatus*♀) used in the experiments were purchased from the Daya Bay Breeding Test Center in Huizhou City, Guangdong Province, China.

2.2 Extraction and purification

Briefly, the pomelo fruitlets were washed, chopped in granular form, and powered by the grinder. Then, the powders were extracted using pectinase and cellulase (2% w/v, pH 6.0, 50 °C, 2 h) with distilled water at a ratio of 1:30 (w/v). After enzyme inactivation and sonication (Wu et al., 2020), the reaction mixture was centrifuged (3622 × g) and the supernatant liquor was concentrated. Subsequently, the collected solution was deproteinized using 10% trichloroacetic acid (Chen et al., 2018), and precipitated with ethanol. Then, the samples were dissolved in deionized water and lyophilized to give the crude polysaccharide, which was next separated using a DEAE-Sepharose Fast Flow chromatography column (2.5 × 60 cm), eluted by ultrapure water and NaCl solution (0.2, 0.5, or 2 M, pH 7.0), and then purified using a Sephadex G-100 column (1.6 cm × 60 cm) (Chen et al., 2019).

2.3 Structural characterization

2.3.1 Fourier transform infrared spectroscopy

Samples (2 mg) were mixed with 200 mg KBr, ground, and then pressed into pellets for FT-IR scanning. Spectra were collected in the frequency range of 4000–400 cm⁻¹.

2.3.2 Molecular weight determination

The molecular weight distribution of YZ-0.5A was analyzed by high performance gel-permeation chromatography (HPGPC) using a Shimadzu LC-10A system linked to a Shimadzu RI-502 (Liu et al., 2018).

2.3.3 Monosaccharide composition and methylation analysis

The monosaccharide composition of YZ-0.5A was analyzed by high performance anion exchange chromatography (HPAEC) with

a CarboPac TM PA20 (3 × 150 mm) column (Dionex, CA, USA) (Liu et al., 2017). Fucose, rhamnose, arabinose, galactose, glucose, xylose, mannose, fructose, galacturonic acid, and glucuronic acid were used as standards (Catal et al., 2008; Song et al., 2019). Methylation analysis of YZ-0.5A was determined by gas chromatography-mass spectrometry using a GCMS-QP2010 system (Shimadzu, Japan) equipped with an RXI-5 SIL ms quartz capillary column (30 m × 0.25 μm × 0.25 mm) according to a method in (Guo et al., 2019).

2.3.4 NMR analysis

The NMR chemical shifts of one-dimensional (¹H, ¹³C, and ¹³C-DEPT-135) and two-dimensional (¹H-¹H COSY, NOESY, ¹³C-¹H-HSQC, and ¹³C-¹H-HMBC) YZ-0.5A were measured using a Bruker 600 MHz spectrometer (Bruker Corp, Fallanden, Switzerland) and are presented in ppm.

2.4 In vitro studies

Primary hepatocytes of the juvenile hybrid grouper were isolated and cultured according to the method of (Zou et al., 2019). The primary hepatocytes were cultured in MEM containing 1% (v/v) penicillin-streptomycin double antibody (negative control) and 10% (v/v) FBS at 25 °C with 5% CO₂. After culturing the hepatocytes for 24, 48, and 72 hours, the YZ0.5-A dosage concentrations were selected for follow-up experiments according to cell viability. The groups and the treatment method were as follows. Control group: hepatocytes alone; model group (LE for 72 h); and recovery group: hepatocytes were treated with LE for 48 h, and then incubated with normal medium for 24 h; YZ0.5-A group: hepatocytes were incubated with LE for 48 h, and then incubated for 24 h with 75, 150, or 300 μg/mL YZ0.5-A). Samples were analyzed after 72 h.

2.5 In vivo study with dietary YZ0.5-A

2.5.1 Diet preparation

The formulation and composition of the basal diets are listed in Table 1. The crude protein, crude lipid, and ash content of this formula are 47.44 ± 0.34%, 14.95 ± 0.03%, and 12.49 ± 0.17%, respectively. Five semi-purified basal diets were supplemented with 0 (control, without extra YZ0.5-A addition), 150 (YZ-0.5-150), 300 (YZ-0.5-300), 600 (YZ-0.5-600), or 1200 (YZ-0.5-1200) mg/kg YZ0.5-A. All the ingredients were ground into powder, mixed according to the proportion, and made into 2-mm pellets with a pelletizer (F-26; South China University of Technology, Guangzhou, China). Then, all diets were air-dried at 40°C until the moisture level reached 4% and stored at -20°C.

2.5.2 Experimental procedures

The experimental procedures were similar to those described in our previous study (Zou et al., 2019). Three hundred juvenile groupers (13.46 ± 0.08 g) were randomly divided into five

TABLE 1 Composition and nutrients in experimental diets (g/kg).

| Ingredient | YZ-0.5-0 | YZ-0.5-150 | YZ-0.5-300 | YZ-0.5-600 | YZ-0.5-1200 |
|----------------------------|----------|------------|------------|------------|-------------|
| Fish meal | 450.00 | 450.00 | 450.00 | 450.00 | 450.00 |
| Soybean meal | 180.00 | 180.00 | 180.00 | 180.00 | 180.00 |
| Flour | 200.00 | 198.50 | 197.00 | 194.00 | 188.00 |
| Soybean oil | 50.00 | 50.00 | 50.00 | 50.00 | 50.00 |
| Fish oil | 50.00 | 50.00 | 50.00 | 50.00 | 50.00 |
| Beer yeast powder | 20.00 | 20.00 | 20.00 | 20.00 | 20.00 |
| Monocalcium phosphate | 10.00 | 10.00 | 10.00 | 10.00 | 10.00 |
| Lecithin | 10.00 | 10.00 | 10.00 | 10.00 | 10.00 |
| Choline chloride (50%) | 5.00 | 5.00 | 5.00 | 5.00 | 5.00 |
| Vitamin C | 5.00 | 5.00 | 5.00 | 5.00 | 5.00 |
| Vitamin and mineral premix | 20.00 | 20.00 | 20.00 | 20.00 | 20.00 |
| YZ0.5-A | 0.00 | 0.15 | 0.30 | 0.60 | 1.20 |
| Nutrient levels (%) | | | | | |
| Moisture | 5.65 | 5.86 | 5.57 | 5.26 | 5.88 |
| Crude protein | 47.44 | 48.04 | 47.12 | 47.35 | 47.40 |
| Crude lipid | 14.95 | 14.90 | 14.94 | 14.91 | 14.88 |
| Ash | 12.49 | 12.13 | 12.08 | 12.11 | 12.14 |

Vitamin and mineral premix provided by Guangzhou Chengyi Aquatic Co., Ltd., China.

experimental groups, with three replicates in each group (15 floating cages). Fish were fed to apparent satiation two times daily at 8:00 and 16:00. The feeding trial lasted for 8 weeks, during which the number of dead fish, the weight of dead fish, and feed consumption were recorded daily. At the end of the feeding trial, fish were fasted for 24 h and euthanized with 100 mg/L MS222 to detect the weight gain (WG) and condition factor (*K*). Blood samples were collected by caudal venipuncture using 2 ml syringes to analyze biochemical indices. After blood withdrawal, the fish were dissected for the calculation of hepatosomatic index (HSI), and viscerosomatic index (VSI). Then, liver samples were removed and stored at -20°C for further analyses. All experimental protocols were approved by the Institutional Animal Care and Use Committee (IACUC) of Zhongkai University of Agriculture and Engineering (ethics code permit number: ZK20180518).

2.6 Sample analysis

2.6.1 Cell viability assay

The viability of hepatocytes treated with YZ0.5-A was evaluated using cell counting kit-8 assays (CCK-8; ABP Biosciences, Beltsville, MD, USA) according to the method used in our previous study (Zou et al., 2018).

2.6.2 Histopathological analysis

Hematoxylin and eosin (H&E) staining on the liver tissue and hepatocytes of hybrid grouper was conducted according to previous methods (Zou et al., 2022). *In vivo* experiment, dissected liver specimens were fixed at 4% neutral buffered formalin and dehydrated in graded ethanol concentrations and impregnated with paraffin. Subsequently, the paraffin-soaked specimens were frozen and cut into 5- μm thickness sections in the cryostat. The sections were stained with hematoxylin and eosin (H&E) for optical examination. *In vitro* experiment, isolated hepatocytes were washed with phosphate buffered saline (PBS), fixed with 4% paraformaldehyde for 20 min, and rinsed in 0.1M PBS \times 4 for 2 min each time. Then staining with H&E was performed after the removal of PBS. A Light microscope (200 \times , MshOt MS60) was used to picture the morphological features of the processed samples.

2.6.3 Histochemical analyses

Liver tissues were embedded in 4% buffered formaldehyde and processed into frozen thickness sections (9- μm) as described in 2.6.2. The sections were then stained with Oil Red O solution. The hepatocytes were fixed as described in 2.6.2, immersed in 60% isopropanol for 3-5s and rinsed in distilled water. The cells were stained for 8-10 min with filtered oil red O in dark, then exhaustively rinsed with water. The nuclei were counterstained

with hematoxylin for 3–5 min. After one further rinse in water, intracellular lipid droplets were observed using microscope (MshOt MS60). The relative area of vacuolation and lipid droplets in stained samples was analyzed by Image-Pro Plus 6.0. stained samples.

2.6.4 Growth performance and morphometric parameters

The initial body weight, final body weight (FBW), WG, feed efficiency (FE), HSI, VSI, K and specific growth rate (SGR) were measured using the following formulae:

Weight gain (WG, %)

$$= \frac{100 \times (\text{final body weight} - \text{initial body weight})}{\text{coninitial body weight}}$$

$$\text{Feed efficiency (FE)} = \frac{\text{wet weight gain (g)}}{\text{dry feed intake (g)}}$$

$$\text{Condition factor (K, g/cm}^3) = \frac{100 \times (\text{body weight, g})}{(\text{body length, cm})^3}$$

$$\text{Viscerosomatic index (VSI, \%)} = \frac{100 \times (\text{viscera weight, g})}{(\text{whole body weight, g})}$$

$$\text{Hepatosomatic index (HSI, \%)} = \frac{100 \times (\text{liver weight, g})}{(\text{whole body weight, g})}$$

specific growth rate (SGR, %)

$$= \frac{100 \times [\ln(\text{Final weight}) - \ln(\text{Initial weight})]}{(\text{Duration})}$$

2.6.5 Chemical analysis

Whole body and muscle moisture were determined using the Kjeldahl method. Crude protein (N \times 6.25) was measured after acid digestion using a Kjeltac 8400 (FOSS, Hilleroed, Denmark). Crude lipid was determined using ether extraction by SoxtecTM 2055 (FOSS, Hoganas, Sweden). The samples were dried in the oven at 150°C for 24 h to measure moisture content. Ash in the whole body, muscle, and diet was measured with a muffle furnace (FO610C; Yamato Scientific Co., Ltd., Tokyo, Japan) at 550°C for 24 h.

2.6.6 Biochemical assays

Biochemical indicators of antioxidation, including CAT, SOD, GR, and GSH-Px activity were evaluated using detection kits (Jiancheng Institute of Biotechnology, Nanjing, China) in a spectrophotometer following the method previously described (Zou et al., 2018).

2.6.7 Cell apoptosis analysis

Apoptotic cells were evaluated by flow cytometric analysis after using Annexin H-APC/7AAD detection kit (Multi sciences, Shanghai, China) following the manufacturer's instructions. Briefly, hepatocytes (1 \times 10⁶ cells) were reseeded in 6-cm dishes

and proceeded with Annexin V-APC/7-AAD double staining, fixed at 28 °C for

15 min, and subsequently stored in ice. Then, cells were analyzed by flow cytometry.

2.6.8 Real-time qPCR

Total RNA was isolated from the liver samples using TRIzol reagent (Invitrogen, Waltham, MA, USA). mRNA quality was measured by spectrophotometry (A₂₆₀:A₂₈₀ ratio) and electrophoresis using 1.2% agarose gels. Then, cDNA was synthesized using an Easy Script First-Strand cDNA Synthesis SuperMix (Transgen Biotech, Beijing, China). The specific primers for each gene are listed in Table 2 (Tan et al., 2018; Zou et al., 2021). The real-time PCR reactions were carried out in a final volume of 20 μ l, using 1 \times Power SYBR Green PCR MasterMix buffer (ABI, USA) on a Step-one PCR amplifier (ABI, USA). Cycling parameters were as follows: 1 min at 94°C, followed by 40 cycles of 10 s at 94°C; 40 cycles of 20 s at 60°C; and 40 cycles of 30 s at 72°C. All assays were carried out in triplicate. The mRNA expression levels were normalized to the geometric mean of the reference genes (β -Actin) using the 2^{- $\Delta\Delta$ Ct} method.

2.7 Statistical analysis

Data were expressed as mean \pm standard deviation of three biological replicates. One way analysis of variance was used to determine significant differences at $P < 0.05$. Linear and quadratic effects of YZ-0.5A supplementation at increasing levels *in vivo* were evaluated using an orthogonal polynomial contrast test. All statistical analyses were conducted using SPSS 11.0 software (SPSS Inc., Chicago, IL, USA).

3 Results and discussion

3.1 Structure analysis

3.1.1 Extraction and purification

The NaCl-soluble polysaccharide YZ-0.5A was extracted from pomelo fruitlets and obtained after deproteinization. The isolated YZ-0.5 was first fractionated with a DEAE-Sepharose Fast Flow chromatography column and eluted with 0.5 M NaCl solution. After Sephadex G-200 gel chromatography, the curve showed that a YZ-0.5A fraction was obtained from YZ-0.5 (Figure 1A). YZ-0.5A is an acidic polysaccharide, as it was eluted with NaCl solution. When the NaCl concentration was increased to 0.5 M, the production of soluble sugar concentration increased to a maximum and then decreased with increasing NaCl.

3.1.2 FT-IR of YZ-0.5A

The FT-IR spectrum of YZ0.5-A is shown in Figure 1B. The broad peak at approximately 3600–3200 cm⁻¹ was due to the stretch vibration of the -OH bond, which was the characteristic polysaccharide peak. The band at 2935 cm⁻¹ was the characteristic

TABLE 2 Primers for qPCR of lipid metabolism related genes.

| Primers | qPCR primers, forward/reverse (5' to 3') |
|----------------|--|
| DGAT2 | F: CATCTTCTGCTTTGGTGCTTTC |
| | R: GCATTTCCCGTCCCGTTA |
| LXR α | F: CAGAAGCAATGCAACAAAAGG |
| | R: TCAGTGAAGTGGGCGAACC |
| G6PD | F: GCTTCACATCCTTGATCTGCTC |
| | R: GCGTTCCTTTCATTCTCCG |
| ME1 | F: GAAGTTGTTCTACCGCTTGCTG |
| | R: AGAGTCTCGTGGTCTCCTGA |
| FAS | F: CGGGTGTCTACATGGGGTG |
| | R: GAATAGCGTGAAGGCGTTT |
| AMPK α | F: CCTCTCGACTTCCGTAGCA |
| | R: CTGCCCCATCCACATCGTTC |
| AMPK β | F: CGGAGGGAGAGCACCAGTAT |
| | R: TGTCTCTGGCTTGGTCACA |
| AMPK γ | F: AACAGACTGGTTCGAGGCAGA |
| | R: AAGCTGTGCCCTCATCTCCA |
| SERBP-1 | F: AGCTGTTTACACACTCCACTCG |
| | R: ACTGTGGAAGCTACAGGGCA |
| SCD1 | F: GCAGAGTTTGTAGCCGGTGT |
| | R: TGCTTCTTGGGTTTGGCTCA |
| SIRT1 | F: CCACTATTAGCAGGCAGTAGGCTT |
| | R: CACTGCAGCGTACAGCGAAT |
| CPT1 | F: TCCTTACCCTGGTCCCTCT |
| | R: CTTTCCATCTGCTGCTCTATCTC |
| LPL | F: TTCAACAGCACCTCCAAAACC |
| | R: GTGAGCCAGTCCACCACGAT |
| ACO1 | F: CGGCATGGACTTCTGTATG |
| | R: CCTGGTGTGGTGTGTGTGT |
| PPAR α | F: CATCGACAATGACGCCCTC |
| | R: GCCGCTATCCCGTAAACAAC |
| β -Actin | F: TACGAGCTGCCTGACGGACA |
| | R: GGCTGTGATCTCCTTCTGC |

DGAT2, acyl CoA diacylglycerol acyltransferase 2; LXR α , liver X receptor α ; G6PD, glucose 6-phosphate dehydrogenase; ME1, malic enzyme 1; FAS, fatty acid synthase; AMPK α , AMPK β , and AMPK γ , three heteromeric complexes of AMPK pathway; SERBP-1, SERPINE1 mRNA binding protein 1; SCD1, Stearoyl-CoA desaturase 1; CPT1, carnitine palmitoyl transferase 1; LPL, lipoprotein lipase; ACO1, acyl-CoA oxidase 1; PPAR α , peroxisome proliferator-activated receptor alpha.

C-H absorption peak. The absorption peak at 1610 cm^{-1} represented N-H stretching vibration (PoMohammadur Dounighi et al., 2015). The absorption bands at 1427, 1338, 1240, and 1016 cm^{-1} represented C-O, C=O, and O-H vibrations (PoMohammadur Dounighi et al., 2015; Amutha et al., 2017). Further, the

characteristic absorption band at 890 cm^{-1} was assigned to the pyran structures, which might be caused by C-H stretching vibration. YZ0.5-A may be a β -terminus differential isomer, but the β -terminus configuration needed to be further determined by nuclear hydrogen and carbon spectra. According to our previous research, the crude polysaccharide extracted from pomelo fruitlets is a residue polymer containing acidic monosaccharides with pyran rings, which is consistent with this result.

3.1.3 Molecular weight

According to the HPGPC analysis, there was only one symmetrical signal peak in the molecular weight profile of the YZ0.5-A fractions (Figure 1C), indicating high sample purity. The estimated average molecular weight of the YZ0.5-A fractions, based on calibration with the standard, was calculated to be 15,332 Da. Previous studies have suggested that biological activity is closely related to molecular weight (Sheng and Sun, 2014). If the molecular weight of the polysaccharide is too small or too large, the molecule usually has no biological activity (Huang et al., 2020). Thus, proper molecular weight distribution can denote good biological activity (Zhang et al., 2016).

3.1.4 Monosaccharide composition

The anion chromatography analysis of 12 standard monosaccharides is shown in Figure 1D and the chromatogram (Figure 1E) revealed five peaks indicating that YZ0.5-A was heterogeneous. Based on the retention time of each monosaccharide, the monosaccharide composition in YZ0.5-A included Rha, Ara, Gal, Glu, and GalA in a molar ratio of 0.088: 0.157: 0.331: 0.123: 0.301. As the previous study regarding the structure-activity relationship of polysaccharide reported, polysaccharides with an MW range of 4000–100,000 Da and a high proportion of GalA and Ara could show appreciable bioactive, like antioxidant activity (Li et al., 2016). Hence, YZ0.5-A with 15,332 Da and containing nearly 45% of GalA and Ara could be postulated to have bioactive potential.

3.1.5 Methylation analysis

Methylated YZ0.5-A was analyzed by gas chromatography-mass spectrometry (GC-MS) to elucidate the types of glycosyl linkages. As summarized in Table 3, GC-MS demonstrated that YZ0.5-A has 11 main types of sugar linkages: terminal Araf, 1,5-linked Araf, terminal Glcp, terminal Galp, 1,2,4-linked Rhap, 1,2-linked Galp, 1,4-linked Glcp, 1,4-linked Galp, 1,6-linked Galp, 1,4,6-linked Glcp, and 1,3,6-linked Galp, with molar percentage ratios of 3.43:22.4:2.63:4.22:8.96:6.8:14.42:17.68:7.65:6.16:5.65, respectively. According to the results in the monosaccharide composition identified by HPAEC analysis, the GC-MS results demonstrated that the major backbone of YZ0.5-A may contain 1,5-linked Araf (22.40%), 1,4-linked Glcp (14.42%), and 1,4-linked Galp (17.68%).

3.1.6 NMR spectroscopy analysis

The 1D NMR spectrum of YZ0.5-A, including ^1H , ^{13}C , and Dept135, is shown in Figures 2A–C. The proton spectrum signals

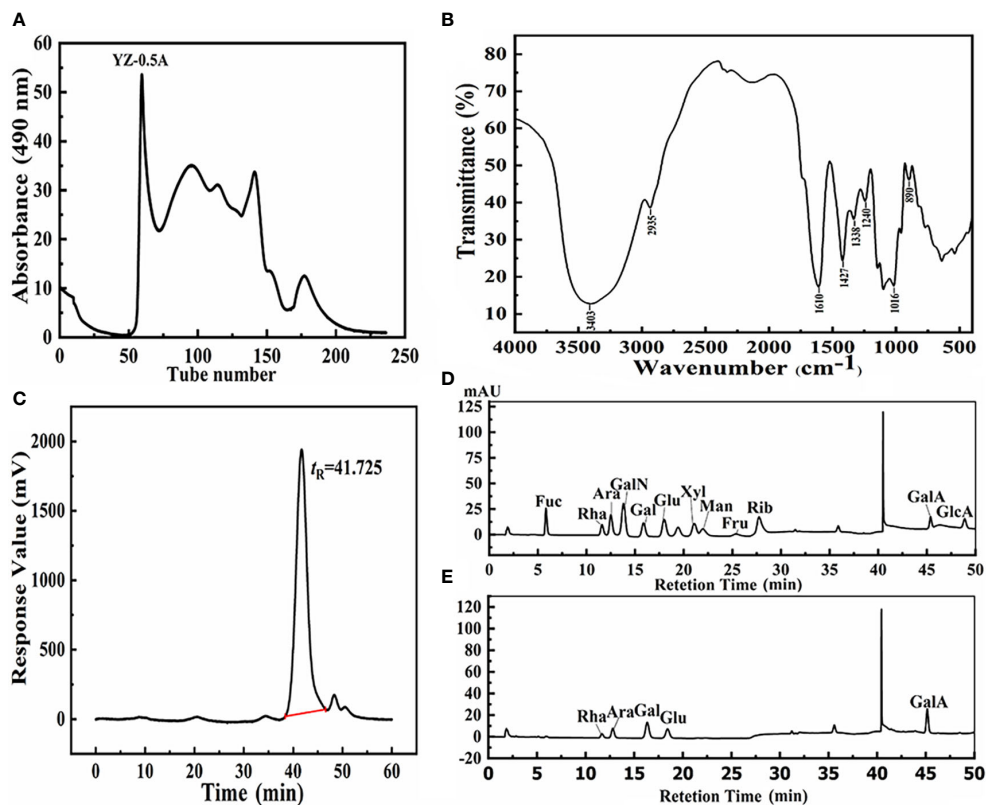


FIGURE 1

Structural information of YZ0.5-A isolated from pomelo fruitlets. (A) Gel permeation chromatogram using a Sephadex G-200 column; (B) FT-IR spectra of YZ0.5-A; (C) HPGPC of YZ0.5-A; (D) HPAEC of monosaccharide standards; (E) HPAEC of YZ0.5-A.

between δ 3.0–5.5 ppm and δ 3.2–4.0 ppm were the sugar ring proton signals (Li et al., 2017), and the main terminal matrix proton peaks, namely, δ 4.40, 4.42, 4.57, 4.58, 4.62, 4.89, 4.97, 5.02, 5.07, 5.09, 5.22, 5.28, and 5.34 ppm, were concentrated in the δ 4.3–5.5-ppm area. The main anomeric carbon signal peaks of δ 108.77, 108.31, 105.52, 105.28, 105.0, 104.58, 104.35, 101.41, 101.14, 101.13, 100.04, 99.7, and 98.44 ppm appeared at the ^{13}C

NMR spectrum (201 MHz, D₂O), which were distributed in the δ 93–105-ppm area. According to the HSQC spectrum (Figure 2D), the aforementioned signals could be classified as $\delta\text{H}/\text{C}$: 5.09/108.31, 5.02/108.77, 4.62/105.28, 4.42/104.35, 4.58/105.52, 4.57/105.00, 4.40/104.58, 5.22/99.70, 4.97/98.44, 5.07/100.04, 5.34/101.14, 4.89/101.41, and 5.28/101.13 ppm labeled as A–M, respectively. The Dept135 spectrum of YZ0.5-A showed inverted peaks at δ 70.6,

TABLE 3 Linkage analyses of YZ0.5-A and its degraded products.

| Methylation sugar | Retention time (min) | Linkage type | Molar ratio (%) |
|-------------------------------|----------------------|----------------|-----------------|
| 2,3,5-Me ₃ -Araf | 9.486 | Araf-(1→ | 3.43 |
| 2,3-Me ₂ -Araf | 14.507 | →5)-Araf-(1→ | 22.40 |
| 2,3,4,6-Me ₄ -GlcP | 16.308 | GlcP-(1→ | 2.63 |
| 2,3,4,6-Me ₄ -GalP | 17.528 | GalP-(1→ | 4.22 |
| 3-Me ₁ -Rhap | 18.351 | →2,4)-Rhap-(1→ | 8.96 |
| 3,4,6-Me ₃ -GalP | 19.094 | →2)-GalP-1→ | 6.80 |
| 2,3,6-Me ₃ -GlcP | 21.045 | →4)-GlcP-(1→ | 14.42 |
| 2,3,6-Me ₃ -GalP | 21.369 | →4)-GalP-(1→ | 17.68 |
| 2,3,4-Me ₃ -GalP | 24.418 | →6)-GalP-(1→ | 7.65 |
| 2,3-Me ₂ -GlcP | 27.395 | →4,6)-GlcP-(1→ | 6.16 |
| 2,4-Me ₂ -GalP | 29.659 | →3,6)-GalP-(1→ | 5.65 |

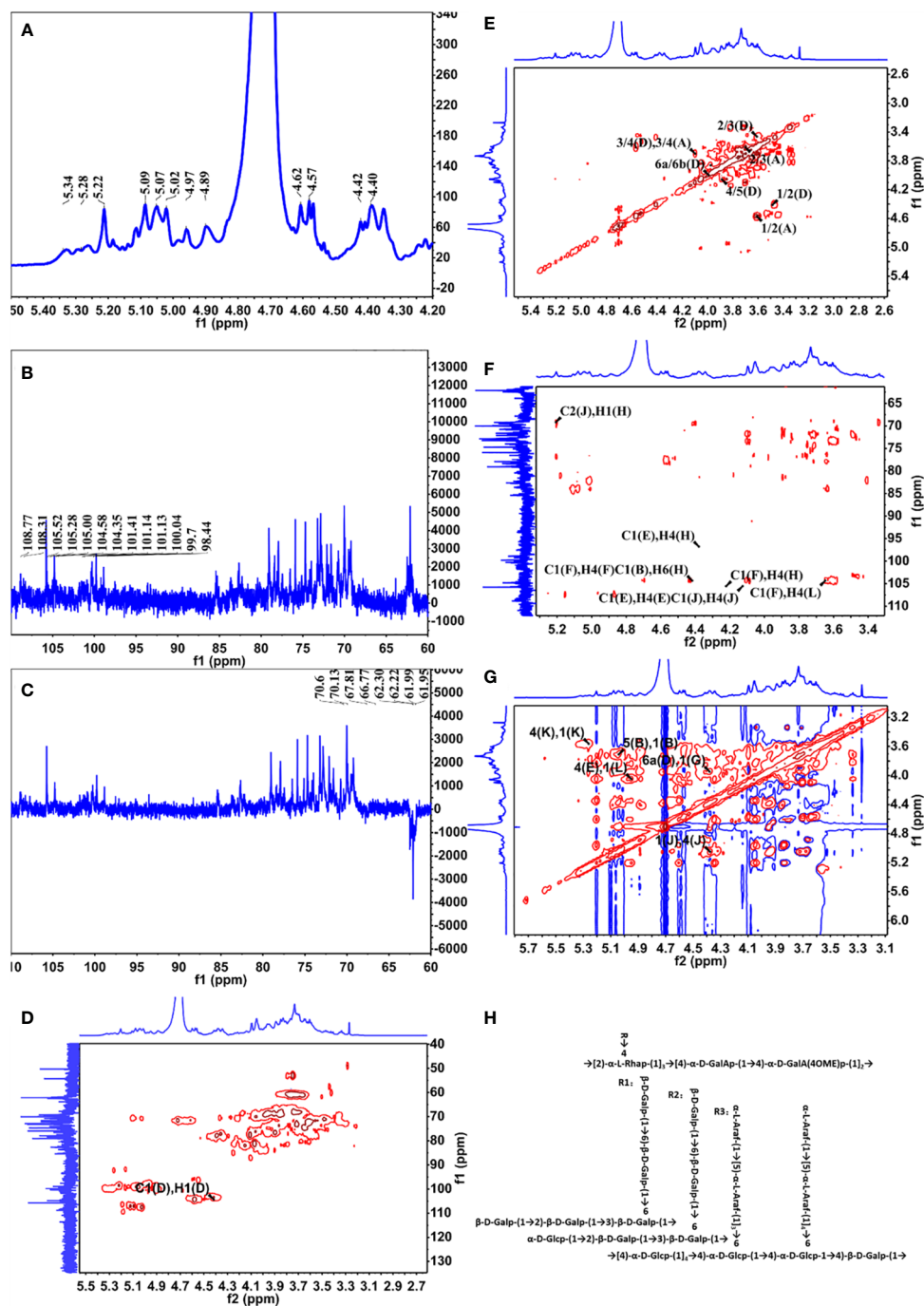


FIGURE 2 NMR spectra of YZ0.5-A. (A) ¹H NMR; (B) ¹³C HMR; (C) DEPT 135; (D) HSQC; (E) COSY; (F) HMBC; and (G) NOESY. (H) Putative structure of YZ0.5-A.

70.13, 67.81, 66.77, 62.3, 62.22, 61.99, 61.99, and 61.95 ppm, indicating the C6 chemical shift.

The anomeric hydrogen signal of residue D was designated as δ4.42 ppm, and its signals of H2-H6a could be obtained from the COSY spectrum (Figure 2E), which are δ4.42, 3.57, 3.68, 4.05, 3.87, and 3.96. Meanwhile, as a reference to the HSQC spectrum (Figure 2D), the corresponding carbon signals of H2-H6a could be inferred to be: 72.23, 81.54, 70.60, 75.25 and 70.60. Therefore, based on these results and the literature, residue D was considered

as →3,6)-Galp-(1→(Hu et al., 2015). In this way, the hydrogen and carbon signals of all other residues could also be obtained and inferred to the possible glycosidic bond. Hence, all glycosidic bonds were determined and assigned, as shown in Table 4.

Some legible cross-peaks between the ¹H and ¹³C signals of different sugar residues could be observed in the HMBC spectrum (Figure 2F), which are: h H1 and j C2, j H1 and j H4, e C1 and e H4, e C1 and h H4, b C1 and l H6, f C1 and d H3 and d C1 and h H4. These cross-peaks corroborated the presence of →2,4)-α-L-Rhap-

TABLE 4 The chemical shift data for related glycosyl residues of YZ0.5-A.

| Residue | Glycosyl linkage | H1 | H2 | H3 | H4 | H5 | H6a/6b |
|---------|--|--------|-------|-------|-------|-------|-----------|
| | | C1 | C2 | C3 | C4 | C5 | C6 |
| A | α -L-Araf-(1 \rightarrow) | 5.09 | 4.07 | 3.90 | 4.02 | 3.67 | 3.78 |
| | | 108.31 | 82.24 | 77.82 | 85.26 | 62.22 | ns |
| B | \rightarrow 5)- α -L-Araf-(1 \rightarrow) | 5.02 | 4.07 | 3.95 | 4.15 | 3.74 | 3.82 |
| | | 108.77 | 82.24 | 78.05 | 83.17 | 67.81 | ns |
| C | β -D-Galp-(1 \rightarrow) | 4.62 | 3.37 | 3.87 | 3.52 | 3.76 | ns |
| | | 105.28 | 73.16 | 70.13 | 75.95 | 62.22 | ns |
| D | \rightarrow 3,6)- β -D-Galp-(1 \rightarrow) | 4.42 | 3.48 | 3.68 | 4.06 | 3.87 | 3.98/4.05 |
| | | 104.35 | 72.23 | 81.54 | 70.60 | 75.25 | 70.60 |
| E | \rightarrow 4)- β -D-Galp-(1 \rightarrow) | 4.58 | 3.61 | 3.71 | 4.11 | 3.65 | 3.72/3.73 |
| | | 105.52 | 73.39 | 74.56 | 78.51 | 76.19 | 61.99 |
| F | \rightarrow 2)- β -D-Galp-(1 \rightarrow) | 4.57 | 3.60 | 3.90 | 4.00 | 3.65 | 3.72/3.73 |
| | | 105.00 | 78.00 | 74.20 | 70.50 | 76.19 | 61.99 |
| G | \rightarrow 6)- β -D-Galp-(1 \rightarrow) | 4.40 | 3.48 | 3.56 | 3.79 | 3.30 | 3.91/3.85 |
| | | 104.58 | 72.23 | 72.69 | 67.81 | 74.32 | 70.13 |
| H | \rightarrow 2,4)- α -L-Rhap-(1 \rightarrow) | 5.22 | 4.07 | 4.04 | 4.36 | 3.72 | 1.22 |
| | | 99.70 | 77.82 | 70.37 | 78.28 | 70.83 | 17.88 |
| I | \rightarrow 4)- α -D-Gal(4OME)Ap-(1 \rightarrow) | 4.97 | ns | 3.87 | 4.23 | 5.71 | ns |
| | | 98.44 | ns | 70.13 | 80.38 | 70.03 | 175.00 |
| J | \rightarrow 4)- α -D-GalAp-(1 \rightarrow) | 5.07 | 3.72 | 3.98 | 4.40 | 4.72 | ns |
| | | 100.04 | 69.4 | 69.78 | 79.24 | 72.43 | 176.66 |
| K | \rightarrow 4)- α -D-Glcp-(1 \rightarrow) | 5.34 | 3.56 | 3.89 | 3.57 | 3.78 | 3.78 |
| | | 101.14 | 72.88 | 74.58 | 78.35 | 72.53 | 61.95 |
| L | \rightarrow 4,6)- α -D-Glcp-(1 \rightarrow) | 4.89 | 3.49 | 3.65 | 3.57 | 3.85 | 3.66 |
| | | 101.41 | 75.73 | 74.02 | 78.20 | 74.60 | 66.77 |
| M | α -D-Glcp-1 \rightarrow | 5.28 | 3.60 | 3.70 | 3.95 | 3.97 | 3.65/3.82 |
| | | 101.13 | 71.94 | 74.03 | 70.61 | 71.68 | 62.30 |

(1 \rightarrow 4)- α -D-GalAp-(1 \rightarrow , \rightarrow 4)- α -D-GalAp-(1 \rightarrow 4)- α -D-GalAp-(1 \rightarrow , \rightarrow 4)- α -D-Glcp-(1 \rightarrow 4)- α -D-Glcp-(1 \rightarrow 4,6)- α -D-Glcp-(1 \rightarrow 4)- β -D-Galp-(1 \rightarrow 4)- β -D-Galp-(1 \rightarrow 2,4)- α -L-Rhap-(1 \rightarrow , \rightarrow 5)- α -L-Araf-(1 \rightarrow 3,6)- α -D-Glcp-(1 \rightarrow , \rightarrow 2)- β -D-Galp-(1 \rightarrow 3,6)- β -D-Galp-(1 \rightarrow , \rightarrow 3,6)- β -D-Galp-(1 \rightarrow 2,4)- α -L-Rhap-(1 \rightarrow . While in the NOESY spectrum (Figure 2G), k H1 and k H4, k H1 and l H4, l H1 and e H4, b H1 and b H5 and g H1 to d H6 were observed, indicating the presence of \rightarrow 4)- α -D-Glcp-(1 \rightarrow 4)- α -D-Glcp-(1 \rightarrow , \rightarrow 4)- α -D-Glcp-(1 \rightarrow 4,6)- α -D-Glcp-(1 \rightarrow , \rightarrow 4,6)- α -D-Glcp-(1 \rightarrow 4)- β -D-Galp-(1 \rightarrow , \rightarrow 5)- α -L-Araf-(1 \rightarrow 5)- α -L-Araf-(1 \rightarrow and \rightarrow 6)- β -D-Galp-(1 \rightarrow 3,6)- β -D-Galp-(1 \rightarrow .

Based on the monosaccharide composition and methylation and NMR spectroscopy analyses, we inferred that the main chain of YZ0.5-A is mainly composed of \rightarrow 2,4)- α -L-Rhap-(1 \rightarrow 4)- α -D-GalAp-(1 \rightarrow 4)- α -D-GalAp-(1 \rightarrow with three branches substituted

at O-4 of \rightarrow 2,4)- α -L-Rhap-(1 \rightarrow . The putative structure of YZ0.5-A is outlined in Figure 2H.

3.2 In vivo study

3.2.1 Whole body and muscle composition

The effect of dietary YZ0.5-A on the composition of the whole body and muscles of hybrid groupers is shown in Table 5. Dietary YZ0.5-A significantly decreased the crude lipid content throughout the whole body ($P < 0.05$). Dietary YZ0.5-A had a significant effect on crude protein and crude lipid levels in the muscles of hybrid groupers ($P < 0.05$). The addition of 300–600 mg/kg YZ0.5-A to feed significantly reduced the overall and muscle lipid content. These results indicate that supplementing YZ0.5-A in feed reduces lipid deposition in fish.

TABLE 5 Effects of YZ0.5-A on whole body and muscle composition in hybrid groupers.

| Items | YZ-0.5-0 | YZ-0.5-150 | YZ-0.5-300 | YZ-0.5-600 | YZ-0.5-1200 | Linear | | Quadratic | |
|-----------------------|---------------------------|----------------------------|----------------------------|----------------------------|----------------------------|--------|----------------|-----------|----------------|
| | | | | | | P | R ² | P | R ² |
| Whole body (%) | | | | | | | | | |
| Moisture | 67.58 ± 0.63 ^a | 68.77 ± 0.17 ^a | 69.80 ± 0.38 ^{ab} | 69.51 ± 0.22 ^{ab} | 71.14 ± 1.74 ^b | 0.002 | 0.708 | 0.007 | 0.754 |
| Crude protein | 17.78 ± 0.45 | 18.10 ± 1.18 | 17.45 ± 0.29 | 18.27 ± 0.62 | 17.22 ± 0.48 | 0.543 | 0.043 | 0.741 | 0.072 |
| Crude lipid | 9.82 ± 0.66 ^b | 9.34 ± 0.47 ^b | 8.32 ± 0.10 ^a | 7.91 ± 0.18 ^a | 8.27 ± 0.22 ^a | 0.002 | 0.637 | 0.010 | 0.643 |
| Ash | 4.57 ± 0.54 | 4.55 ± 0.61 | 4.55 ± 0.41 | 4.36 ± 0.06 | 4.45 ± 0.33 | 0.646 | 0.028 | 0.222 | 0.349 |
| Muscle (%) | | | | | | | | | |
| Moisture | 75.20 ± 0.29 ^b | 75.01 ± 0.32 ^{ab} | 75.02 ± 0.26 ^{ab} | 73.83 ± 0.85 ^a | 74.34 ± 1.14 ^{ab} | 0.036 | 0.295 | 0.036 | 0.295 |
| Crude protein | 20.25 ± 0.25 ^a | 21.04 ± 0.57 ^{ab} | 21.63 ± 0.63 ^{bc} | 22.56 ± 0.45 ^c | 22.08 ± 0.22 ^c | 0.001 | 0.639 | 0.003 | 0.661 |
| Crude lipid | 2.44 ± 0.05 ^c | 2.31 ± 0.06 ^{bc} | 2.02 ± 0.16 ^a | 2.08 ± 0.06 ^{ab} | 2.19 ± 0.06 ^{ab} | 0.017 | 0.533 | 0.002 | 0.832 |
| Ash | 1.53 ± 0.03 ^{ab} | 1.45 ± 0.02 ^a | 1.62 ± 0.07 ^b | 1.61 ± 0.10 ^b | 1.64 ± 0.08 ^b | 0.145 | 0.221 | 0.246 | 0.296 |

Values are means ± SD (n = 6) of three replicates. Means in the same row with different superscripts are significantly different ($P < 0.05$). Orthogonal polynomials were used to evaluate linear and quadratic responses to the levels of YZ-0.5A treatments.

3.2.2 Growth performance, feed utilization, morphological parameters and histochemical examination

Previous studies showed that the appropriate lipid content of the juvenile hybrid grouper feed is 7%–13% (Jiang et al., 2016). When the fat content in the diet of hybrid grouper reaches 15%, there is significant fat deposition in the liver or visceral fat tissue in farmed fish (Jia et al., 2017; Zhang et al., 2019a). The effects of YZ0.5-A on the growth performance, feed utilization, and morphological parameters of hybrid groupers fed by a high-fat diet (HFD) are shown in Table 6. The WG of hybrid groupers in the YZ-0.5-600 groups was significantly higher than those in the YZ-0.5-0 group ($P < 0.05$). Except for that in the YZ-0.5-1200 group, the FE of the YZ-0.5-0 group was lower than that of the other experimental groups ($P < 0.05$). HSI, VSI, and K were all decreased, albeit with varying degrees, in the YZ0.5-A treated groups (particularly in YZ-0.5-600 group) compared with the

control group ($P < 0.05$). The decreases of VSI and HSI might be due to the loss of lipid in the liver, which was confirmed by the performance of the Oil Red O-stained liver sections (Figure 3B). The lipid droplet clusters in the YZ-0.5-300, -600, and -1200 groups was reduced relative to the YZ-0.5-0 group. Collectively, these results suggest that YZ0.5-A has a positive effect on growth performance and prevents lipid accumulation and liver enlargement in fish.

3.2.3 Expression of lipid accumulation-related genes *in vivo*

We further assessed the lipid-lowering effect of YZ0.5-A in HFD-fed hybrid grouper using RT-qPCR. As shown in Figure 3C, the expression of diacylglycerol O-acyltransferase 2 (DGAT2), glucose-6-phosphate dehydrogenase (G6PD), malic enzyme 1 (ME1), and fatty acid synthase (FAS), genes related to lipid synthesis (Zou et al., 2019), exhibited no difference in the YZ-0.5-150 to -300 groups but

TABLE 6 Effects of dietary heteroglycan (YZ0.5-A) on growth performance, feed utilization, and morphometric parameters in hybrid groupers.

| Item | YZ-0.5-0 | YZ-0.5-150 | YZ-0.5-300 | YZ-0.5-600 | YZ-0.5-1200 | Linear | | Quadratic | |
|------------------------|----------------------------|-----------------------------|----------------------------|-----------------------------|----------------------------|--------|----------------|-----------|----------------|
| | | | | | | P | R ² | P | R ² |
| IBW (g) | 13.59 ± 0.45 | 13.44 ± 0.04 | 13.37 ± 0.06 | 13.49 ± 0.45 | 13.44 ± 0.05 | 0.487 | 0.041 | 0.477 | 0.043 |
| FBW (g) | 54.23 ± 1.59 | 52.10 ± 4.29 | 54.58 ± 0.40 | 57.07 ± 1.85 | 54.04 ± 1.01 | 0.355 | 0.072 | 0.653 | 0.075 |
| WG (%) | 312.57 ± 7.41 ^a | 305.46 ± 2.46 ^{ab} | 308.34 ± 1.07 ^a | 323.15 ± 12.04 ^b | 302.08 ± 6.75 ^a | 0.850 | 0.004 | 0.221 | 0.315 |
| SGR (%) | 2.47 ± 0.11 | 2.42 ± 0.14 | 2.52 ± 0.01 | 2.58 ± 0.05 | 2.49 ± 0.03 | 0.425 | 0.054 | 0.721 | 0.058 |
| FE (%) | 95.45 ± 0.97 ^{ab} | 96.88 ± 0.82 ^b | 99.11 ± 0.33 ^c | 100.19 ± 0.58 ^c | 93.23 ± 3.31 ^a | 0.843 | 0.003 | 0.121 | 0.319 |
| HSI (%) | 3.30 ± 0.11 ^d | 3.07 ± 0.01 ^{cd} | 2.48 ± 0.10 ^{ab} | 2.13 ± 0.28 ^a | 2.77 ± 0.07 ^{bc} | 0.113 | 0.196 | 0.131 | 0.309 |
| VSI (%) | 12.46 ± 0.49 ^c | 11.55 ± 0.13 ^b | 11.44 ± 0.01 ^b | 10.59 ± 0.34 ^a | 11.87 ± 0.04 ^b | 0.435 | 0.052 | 0.712 | 0.060 |
| K (g/cm ³) | 1.93 ± 0.01 ^d | 1.78 ± 0.03 ^{bc} | 1.83 ± 0.06 ^{cd} | 1.62 ± 0.06 ^a | 1.70 ± 0.02 ^{ab} | 0.120 | 0.189 | 0.137 | 0.303 |

Values are means ± SD (n=6) of three replicates. Means in the same row with different superscripts indicate significant differences ($P < 0.05$). Orthogonal polynomials were used to evaluate linear and quadratic responses to the levels of YZ-0.5A treatments. IBW, initial body weight; FBW, final body weight; WG, weight gain; SGR, specific growth rate; FE, feed efficiency; HSI, hepatosomatic index; VSI, viscerosomatic index; K, condition factor.

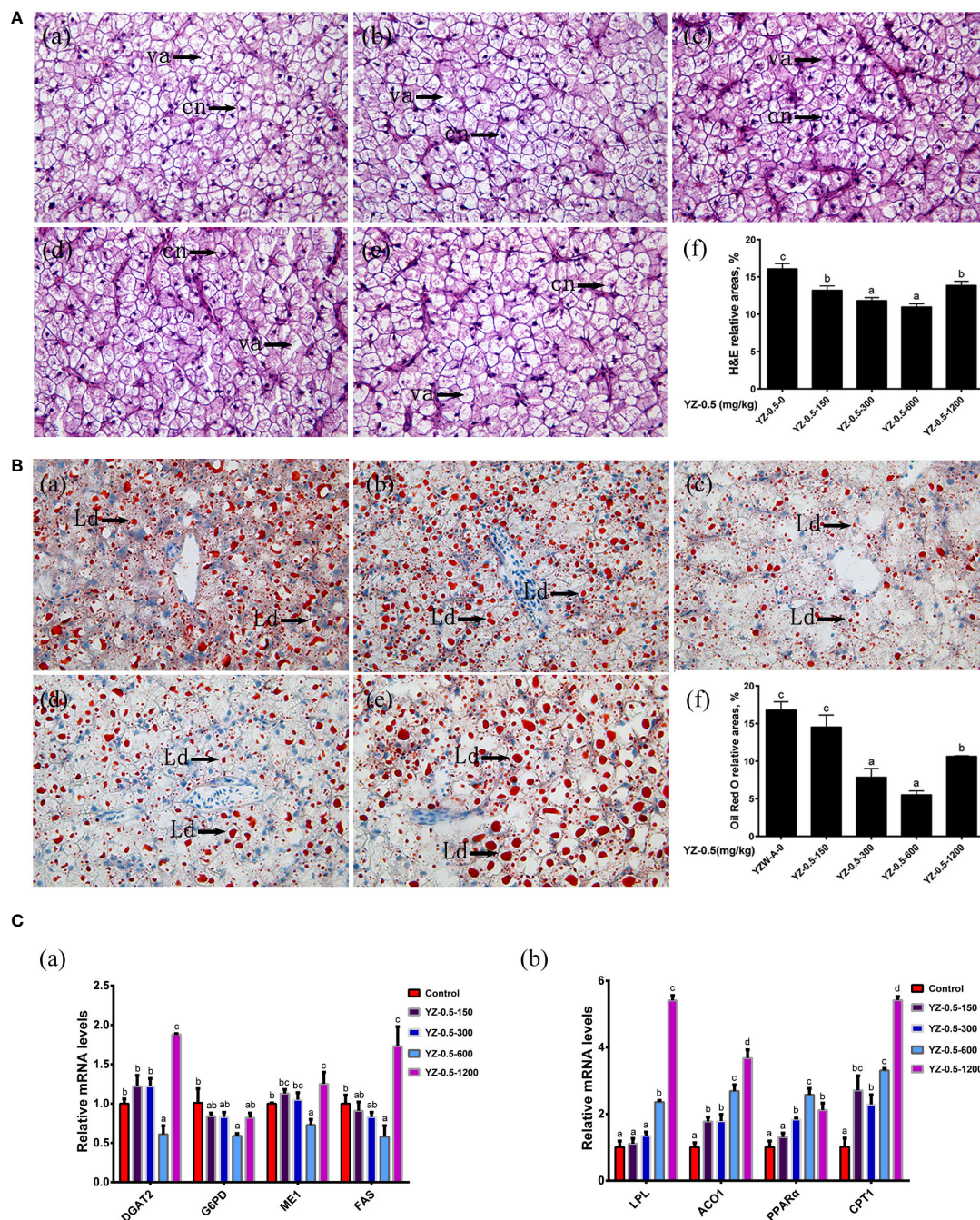


FIGURE 3

Effect of YZ0.5-A on the liver *in vivo*. (A) Histology (100x, cn: cell nucleus, va: vacuolation). (a) Liver from fish fed 0 mg/kg YZ-0.5A (YZ-0.5-0); (b) Liver from fish fed 150 mg/kg YZ-0.5A (YZ-0.5-150); (c) Liver from fish fed 300 mg/kg YZ-0.5A (YZ-0.5-300); (d) Liver from fish fed 600 mg/kg YZ-0.5A (YZ-0.5-600); (e) Liver from fish fed 1200 mg/kg YZ-0.5A (YZ-0.5-1200); (f) Relative areas for hepatic vacuoles in H&E staining. (B) Histochemistry (Oil Red O staining, 400x, Ld: lipid droplet). (a) Liver from fish fed 0 mg/kg YZ-0.5A (YZ-0.5-0); (b) Liver from fish fed 150 mg/kg YZ-0.5A (YZ-0.5-150); (c) Liver from fish fed 300 mg/kg YZ-0.5A (YZ-0.5-300); (d) Liver from fish fed 600 mg/kg YZ-0.5A (YZ-0.5-600); (e) Liver from fish fed 1200 mg/kg YZ-0.5A (YZ-0.5-1200); (f) Relative areas for lipid droplets in Oil Red O staining. Lipids appear red, and nuclei appear blue after staining with Oil Red O. (C) Gene expression *in vivo*. Means in the same row with different superscripts are significantly different ($P < 0.05$).

significantly declined in the YZ-0.5-600 group compared with that in the control ($P < 0.05$). Contrarily, the expression of the above factors was reversely elevated in the fish supplemented with 1200 mg/kg YZ0.5-A ($P < 0.05$), inferring that a specific concentration range of YZ0.5-A could inhibit lipid generation, while a high dose treatment may result in an adverse effect. In contrast, the mRNA expression of

the lipolysis-related genes: lipoprotein esterase, Aconitase 1 (ACO1), peroxisome proliferator-activated receptor alpha (PPAR α), and carnitine palmitoyltransferase 1 (CPT1) (Tan et al., 2019) was also investigated, and the expression was mostly enhanced after the addition of YZ0.5-A ($P < 0.05$). These results imply that treatment with YZ0.5-A improves lipid utilization in fish under HFD feeding.

3.3 In vitro study

3.3.1 Cell viability

To determine the optimal YZ0.5-A treatment time and concentration for hepatocytes and to investigate the YZ0.5-A concentration that mitigates hepatocyte viability after treatment with 2 mL/L 20% LE, we incubated hepatocytes with different YZ0.5-A concentrations for 24, 48, and 72 h. As shown in Figure 4A, all YZ0.5-A concentrations (except 150 and 300 µg/mL) decreased hepatocyte survival after 24 h. However, with

extended culture time, the effect was changed. Cell viability was stable in the YZ0.5-A groups by 48h. While the obvious reduction of viability was observed in cells treated YZ0.5-A with concentration beyond 300 µg/mL compared with that in the control group by 72 h ($P < 0.05$). Thus, we chose these three concentrations as the low-, medium-, and high-dose groups, respectively, for 24-h cell incubation. Compared with that in the control group, the results showed that hepatocyte viability of the model group significantly decreased ($P < 0.05$), while hepatocyte viability in the recovery group was significantly increased compared to that in the model

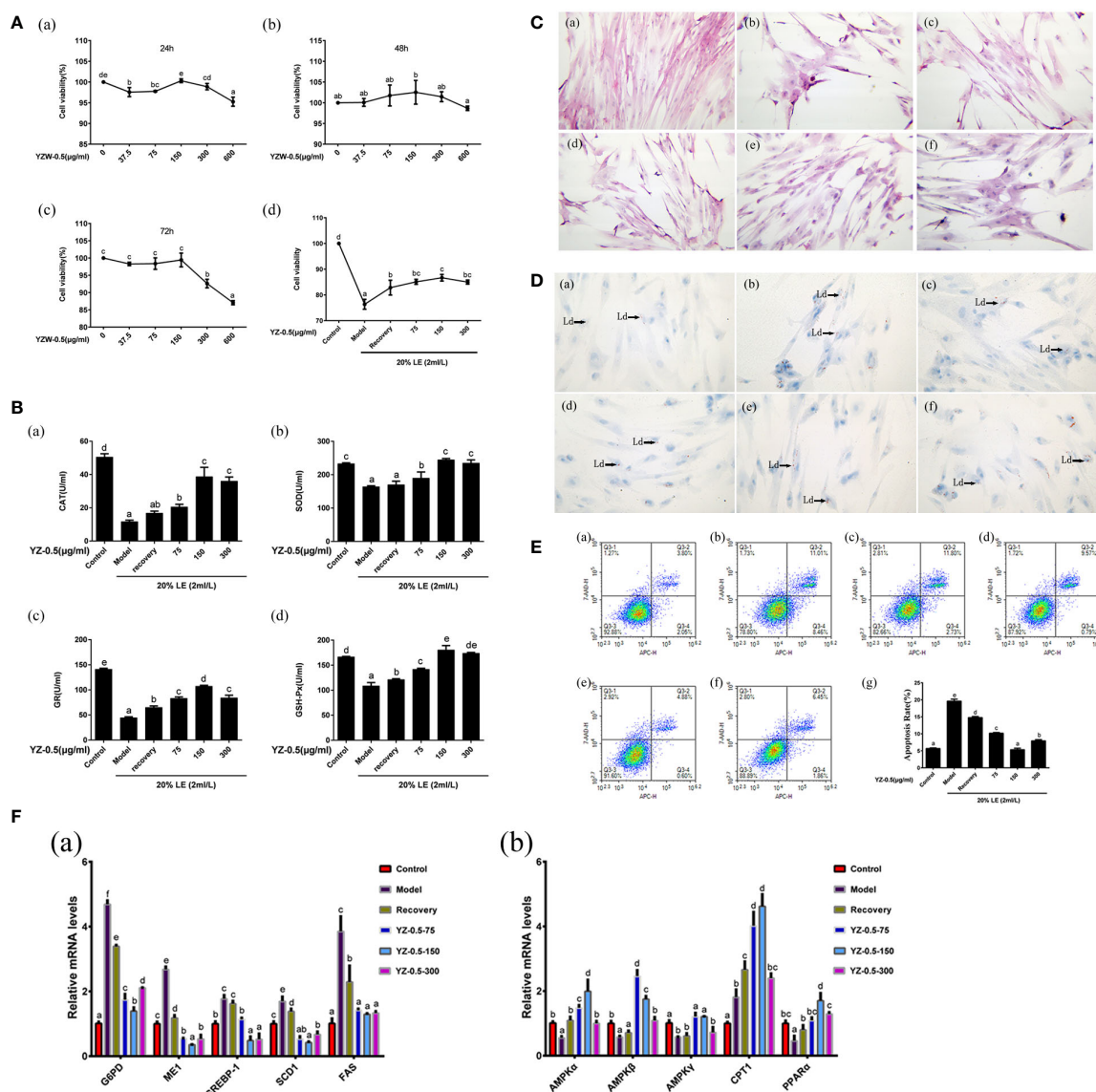


FIGURE 4 Effect of YZ0.5-A on lipid accumulation and antioxidant activity of primary hepatocytes *in vitro*. **(A)** Cell viability. **(B)** The levels of antioxidant enzymes. **(C)** Morphological changes (100x). **(a)** Control: hepatocytes neither treated with 20% lipid emulsion (LE) (2 mL/L) nor YZ0.5-A; **(b)** Model: hepatocytes treated with 20% LE (2 mL/L) alone for 72h; **(c)** Recovery group: hepatocytes treated with 20% LE (2 mL/L) for 48h, then incubated with normal medium for 24 h; **(d)** YZ0.5-A (75 µg/ml) + 20% LE (2 mL/L); **(e)** YZ0.5-A (150 µg/ml) + 20% LE (2 mL/L); **(f)** YZ0.5-A (300 µg/ml) + 20% LE (2 mL/L); **(D)** Histochemistry (Oil Red O staining, 400x; Ld: lipid droplet.) **(a)** Control: hepatocytes neither treated with 20% lipid emulsion (LE) (2 mL/L) nor YZ0.5-A; **(b)** Model: hepatocytes treated with 20% LE (2 mL/L) alone for 72h; **(c)** Recovery group: hepatocytes treated with 20% LE (2 mL/L) for 48h, then incubated with normal medium for 24 h; **(d)** YZ0.5-A (75 µg/ml) + 20% LE (2 mL/L); **(e)** YZ0.5-A (150 µg/ml) + 20% LE (2 mL/L); **(f)** YZ0.5-A (300 µg/ml) + 20% LE (2 mL/L); **(E)** Apoptosis, Q1: dead cells; Q2: early apoptotic cells; Q3: living cells; Q4: late apoptotic and necrotic cells. **F:** mRNA levels in primary hepatocytes. Means in the same row with different superscripts are significantly different ($P < 0.05$).

group ($P < 0.05$). Viability was also remarkably decreased compared to that in the YZ-0.5-150 group ($P < 0.05$). Compared with that in the model group, the survival rate of the recovery group was increased, but compared to that in the YZ0.5-150 group, the survival rate was significantly decreased ($P < 0.05$). Therefore, 75, 150, and 300 $\mu\text{g/mL}$ YZ0.5-A was used for subsequent tests.

3.3.2 Histological and histochemical examination of hepatocytes

H&E staining was used to analyze the hepatocyte structure (Figure 4C). In the control group, the hepatocyte nuclei were normal and neatly arranged. In the model group, the cell structure was destroyed, and vacuoles formed. In the recovery group, the cell state recovered slightly, and the structural damage improved. YZ0.5-A addition reduced the amount of hepatic cytoplasmic vacuolation, and the disrupted cell morphology was alleviated. Further, YZ0.5-A reduced the number of lipid droplets in hepatocytes. The Oil Red O-stained area in the YZ0.5-150 group were smaller than that in other groups (Figure 4D). Moreover, the morphological changes shown with H&E and Oil Red O staining were similar to those in the *in vivo* experiments (Figures 3A, B), giving further support to the therapeutic function of YZ0.5-A in morphological lesions inflicted by excessive lipid administration. Additionally, these results were in agreement with our previous hybrid grouper study that investigated another plant extract, Radix Bupleuri (Zou et al., 2019).

3.3.3 YZ0.5-A alleviates the hepatic steatosis caused by LE via the AMP-activated protein kinase pathway

Lipids play a key role in growth and development. In fish, excessive lipid deposition in the body, especially in the liver, reduces growth rate and causes serious health problems, which poses a serious threat to the sustainable development of aquaculture (Yu et al., 2021). In the present study, as exhibited in Figure 4F, YZ0.5-A treatment significantly offset the LE-induced increase in the mRNA expression of sterol regulatory element-binding protein-1c (SREBP-1c), a transcriptional factor that is conducive to synthesizing lipids, and its functional downstream target, FAS (Ma et al., 2020). Moreover, the transcriptional levels of other genes related to lipid synthesis (G6PD and ME1) were also markedly suppressed in the YZ0.5-A treatment groups relative to the model and recovery group ($P < 0.05$). PPAR α , an important transcriptional factor which could reportedly upregulate the gene expression of the lipid oxidation-related enzyme CPT1, thus promoting lipolysis (Tao et al., 2019). Compared with those in the non-YZ0.5-A treated group, the expressions of PPAR α and CPT1 were markedly enhanced in the YZ0.5-A treated group ($P < 0.05$). These findings indicated that YZ0.5-A shows its therapeutic effect against hepatic steatosis by intensifying fatty acid synthesis while promoting fatty acid utilization. The above performance with H&E and oil red O staining morphologically confirmed this conclusion.

AMPK, a heterotrimer comprised of an α -, β -, and γ -subunits, is a well-documented target of many therapeutic regimens for fatty liver disease (Smith et al., 2016). Specifically, AMPK activation plays

a critical role in regulating lipid metabolism by suppressing SERBP-1c (Sharma et al., 2020). It has been also reported that activation of AMPK could trigger PPAR α and thus improve fatty acid oxidation (Cheng et al., 2015). In this study, the LE-induced reductions in the mRNA expression of AMPK- α -, β -, and γ -in the model group were significantly replenished in the YZ0.5-A-treated groups, particularly at 75 and 150 $\mu\text{g/mL}$ (Figure 4F; $P < 0.05$). Considering the gene expression changes noted in the previous paragraph, these results suggest that YZ0.5-A may influence the activity of AMPK and secondarily its downstream target lipid metabolism-related genes, hence mitigating LE-induced hepatic steatosis.

3.3.4 YZ0.5-A ameliorates oxidative stress and apoptosis inflicted by irregular lipid metabolism

Recent research has shown that lipid accumulation propels the onset of oxidative stress and thus impairs the antioxidant system, which is mainly manifested as a suppressed indicator of antioxidative enzymes (Hong and Lee, 2009). Accordingly, our experiment exhibited a similar effect, as LE challenges cause a reduction in the enzymatic activities of CAT, SOD, GR, and GSH-Px (Figure 4B; $P < 0.05$). Furthermore, apoptosis is regarded as a mechanism involved in the pathophysiologic progress of liver injury induced by excessive lipid deposition, which has occurred in various hepatocyte models, including mice (Xiao et al., 2013), chicken (Ma et al., 2020) and fish (Zhang et al., 2019b). In line with previous investigations, an obvious elevation in the apoptotic rate detected by flow cytometry could be observed in the model and recovery groups relative to that in the control (Figure 4E; $P < 0.05$). Noticeably, the aforesaid pathological performance was significantly reserved in the subsequent experiment with the supplementation of YZ0.5-A (especially at 150 $\mu\text{g/mL}$), indicating its protective effect on the onset of oxidative stress and apoptosis induced by irregular lipid metabolism.

4 Conclusion

In this study, the polysaccharide YZ0.5-A was isolated from pomelo fruitlets. The yield was 9.5%. Based on the monosaccharide, methylation, FT-IR, and NMR spectrum analysis results, YZ0.5-A was identified as a 15332 Da heteropolysaccharide which is mainly composed of 1,5-linked Araf (22.40%), 1,4-linked Glcp (14.42%), and 1,4-linked Galp (17.68%). The main chain is speculated to be $\rightarrow 2,4$ - α -L-Rhap-(1 \rightarrow 4)- α -D-GalAp-(1 \rightarrow 4)- α -D-GalAp-(1 \rightarrow). The results of the *in vivo* study demonstrated for the first time in fish that dietary YZ0.5-A has a positive effect on growth performance and fat loss. Additionally, the *in vitro* experiments indicated that YZ0.5-A may alleviate unwanted lipid accumulation in fish liver, and further inhibit oxidative stress and cell apoptosis. Collectively, the study findings indicated that YZ0.5-A appreciably offset the undesirable outcomes originating from HFD feeding, which not only increases the acceptability of feeding HFD to farmed fish but also provides a new prospective for the reutilization of wasted pomelo fruitlets.

Data availability statement

The raw data supporting the conclusions of this article will be made available by the authors, without undue reservation.

Ethics statement

All experimental protocols were approved by the Institutional Animal Care and Use Committee (IACUC) of Zhongkai University of Agriculture and Engineering (ethics code permit number: ZK20180518). Written informed consent was obtained from the owners for the participation of their animals in this study.

Author contributions

CZ, HL, and GX contributed to the conception and design of the study. CZ and HL took samples of experimental animals. CZ, HL, and YF performed and analyzed all the other experiments. YF and NL wrote the manuscript with support from all authors. LL contributed to the revising of the manuscript. All authors contributed to the article and approved the submitted version.

References

- Amutha, D., Sivasakthi, J., Gubendran, D., Dhanasekaran, P., and Imayatharasi, R. (2017). Studies on metal chelating property and pharmaceutical applications of curcumin metal complex. *IOSR J. Pharm. Biol. Sci.* 12 (3), 72–77. doi: 10.9790/3008-1203017277
- Benhura, M. A. N., and Chidewe, C. (2002). Some properties of a polysaccharide preparation that is isolated from the fruit of *Cordia abyssinica*. *Food Chem.* 76 (3), 343–34. doi: 10.1016/S0308-8146(01)00282-5
- Cao, X., Dai, Y., Liu, M., Yuan, X., and Wang, C. (2019). BBA - molecular and cell biology of lipids high-fat diet induces aberrant hepatic lipid secretion in blunt snout bream by activating endoplasmic reticulum stress-associated IRE1 / XBP1 pathway. *BBA Mol. Cell Biol. Lipids* 1864, 213–223. doi: 10.1016/j.bbalip.2018.12.005
- Catal, T., Li, K., Bermek, H., and Liu, H. (2008). Electricity production from twelve monosaccharides using microbial fuel cells. *J. Power Sources* 175, 196–200. doi: 10.1016/J.JPOWSOUR.2007.09.083
- Cha, J. Y., Cho, Y. S., Kim, I., Anno, T., Rahman, S. M., and Yanagita, T. (2001). Effect of hesperetin, a citrus flavonoid, on the liver triacylglycerol content and phosphatidate phosphohydrolase activity in orotic acid-fed rats. *Plant Foods Hum. Nutr.* 56, 349–358. doi: 10.1023/A:1011884200848
- Chen, L., Huang, G., and Hu, J. (2018). Preparation, deproteinization, characterisation, and antioxidant activity of polysaccharide from cucumber (*Cucumis sativus* L.). *Int. J. Biol. Macromol.* 108, 408–41. doi: 10.1016/j.ijbiomac.2017.12.0341
- Chen, W., Zhu, X., Ma, J., Zhang, M., and Wu, H. (2019). Structural elucidation of a novel pectin-polysaccharide from the petal of *Saussurea laniceps* and the mechanism of its anti-HBV activity. *Carbohydr. Polym.* 223, 115077. doi: 10.1016/J.CARBPOL.2019.115077
- Cheng, K. T., Wang, Y. S., Chou, H. C., Chang, C. C., Lee, C. K., and Juan, S. H. (2015). Kinsenoside-mediated lipolysis through an AMPK-dependent pathway in C3H10T1/2 adipocytes: Roles of AMPK and PPAR α in the lipolytic effect of kinsenoside. *Phytomedicine* 22, 641–647. doi: 10.1016/j.phymed.2015.04.001
- Dai, Y. J., Cao, X. F., Zhang, D. D., Li, X. F., Liu, W. B., and Jiang, G. Z. (2019). Chronic inflammation is a key to inducing liver injury in blunt snout bream (*Megalobrama amblycephala*) fed with high-fat diet. *Dev. Comp. Immunol.* 97, 28–37. doi: 10.1016/j.dci.2019.03.009
- Guo, H., Zhang, W., Jiang, Y., Wang, H., Chen, G., and Guo, M. (2019). Physicochemical, structural, and biological properties of polysaccharides from dandelion. *Molecules* 24 (8), 1485. doi: 10.3390/MOLECULES24081485
- Hong, J. H., and Lee, I. S. (2009). Effects of *Artemisia capillaris* ethyl acetate fraction on oxidative stress and antioxidant enzyme in high-fat diet induced obese mice. *Chem. Biol. Interact.* 179, 88–93. doi: 10.1016/j.cbi.2008.12.002
- Hu, H., Liang, H., and Wu, Y. (2015). Isolation, purification and structural characterization of polysaccharide from *Acanthopanax brachypus*. *Carbohydr. Polym.* 127, 94–100. doi: 10.1016/J.CARBPOL.2015.03.066
- Huang, S., Chen, F., and Cheng, H. (2020). Modification and application of polysaccharide from traditional Chinese medicine such as *Dendrobium officinale*. *Int. J. Biol. Macromol.* 157, 385–393. doi: 10.1016/J.IJBIOMAC.2020.04.141
- Jia, R., Cao, L. P., Du, J. L., He, Q., Gu, Z. Y., Jeney, G., et al. (2020). Effects of high-fat diet on antioxidative status, apoptosis and inflammation in liver of tilapia (*Oreochromis niloticus*) via Nrf2, TLRs and JNK pathways. *Fish. Shellfish Immunol.* 104, 391–401. doi: 10.1016/j.fsi.2020.06.025
- Jia, Y., Jing, Q., Niu, H., and Huang, B. (2017). Ameliorative effect of vitamin e on hepatic oxidative stress and hyp immunity induced by high-fat diet in turbot (*Scophthalmus maximus*). *Fish. Shellfish Immunol.* 67, 634–642. doi: 10.1016/j.fsi.2017.06.056
- Jiang, S., Wu, X., Luo, Y., Wu, M., Lu, S., Jin, Z., et al. (2016). Optimal dietary protein level and protein to energy ratio for hybrid grouper (*Epinephelus fuscoguttatus* ♀ × *epinephelus lanceolatus* ♂) juveniles. *Aquaculture* 465, 28–36. doi: 10.1016/J.AQUACULTURE.2016.08.030
- Khursheed, R., Singh, S. K., Wadhwa, S., Gulati, M., and Awasthi, A. (2020). Therapeutic potential of mushrooms in diabetes mellitus: Role of polysaccharides. *Int. J. Biol. Macromol.* 164, 1194–1205. doi: 10.1016/J.IJBIOMAC.2020.07.145
- Li, Z., Nie, K., Wang, Z., and Luo, D. (2016). Quantitative structure activity relationship models for the antioxidant activity of polysaccharides. *PLoS One* 11, 1–22. doi: 10.1371/journal.pone.0163536
- Li, X., Zhang, B., Li, J., Zhou, J., He, X., Ye, L., et al. (2017). Purification, characterization, and complement fixation activity of acidic polysaccharides from *Tuber sinoestivum*. *LWT Food Sci. Technol.* 85, 82–88. doi: 10.1016/J.LWT.2017.07.006

Funding

This work was supported by the Guangdong Provincial Natural Science Foundation Project [grant number 2019A1515011283].

Acknowledgments

The authors gratefully acknowledge the assistance of Yangzhou BoRui Saccharide Biotech Co. Ltd. for data analysis. We would also like to thank Editage for their language suggestions.

Conflict of interest

The authors declare that the research was conducted in the absence of any commercial or financial relationships that could be construed as a potential conflict of interest.

Publisher's note

All claims expressed in this article are solely those of the authors and do not necessarily represent those of their affiliated organizations, or those of the publisher, the editors and the reviewers. Any product that may be evaluated in this article, or claim that may be made by its manufacturer, is not guaranteed or endorsed by the publisher.

- Liang, D., Wang, J., Warson Ray, G., Yang, Q., Tan, B., Dong, X., et al. (2020). Effects of different dietary levels of soybean protein hydrolysates on the growth performance, antioxidant capacity and relative mRNA expression levels of juvenile hybrid grouper (*Epinephelus fuscoguttatus* ♀ × *epinephelus lanceolatus* ♂). *Aquac. Nutr.* 26, 1857–1870. doi: 10.1111/anu.13134
- Liu, Y., Tong, B., Wang, S., Li, G., Tan, Y., Yu, H., et al. (2021). A mini review of yu-ping-feng polysaccharides: Their biological activities and potential applications in aquaculture. *Aquac. Rep.* 20, 100697. doi: 10.1016/j.aqrep.2021.100697
- Liu, H. N., Wu, H., Tseng, Y. J., Chen, Y. J., Zhang, D. Y., Zhu, L., et al. (2018). Serum microRNA signatures and metabolomics have high diagnostic value in gastric cancer. *BMC Cancer* 109 (4), 1185–1194. doi: 10.1186/S12885-018-4343-4
- Liu, A., Yu, J., Ji, H., Zhang, H., and Zhang, Y. (2017). Extraction of a novel cold-water-soluble polysaccharide from *Astragalus membranaceus* and its antitumor and immunological activities. *Molecules* 23 (1), 62. doi: 10.3390/MOLECULES23010062
- Ma, H., Li, L., Chu, X., Yao, Y., Cao, J., and Li, Q. (2020). (-)-Hydroxycitric acid alleviates oleic acid-induced steatosis, oxidative stress, and inflammation in primary chicken hepatocytes by regulating amp-activated protein kinase-mediated reactive oxygen species levels. *J. Agric. Food Chem.* 68, 11229–11241. doi: 10.1021/acs.jafc.0c04648
- PoMohammadur Dounighi, N., Mehrabi, M., Avadi, M. R., Zolfagharian, H., and Rezayat, M. (2015). Preparation, characterization and stability investigation of chitosan nanoparticles loaded with the *Echis carinatus snake venom* as a novel delivery system. *Arch. Razi Inst.* 70, 269–277. doi: 10.7508/ARI.2015.04.007
- Sharma, A., Anand, S. K., Singh, N., Dwivedi, U. N., and Kakkar, P. (2020). Berberine induced AMPK activation regulates mTOR/SREBP-1c axis and Nrf2/ARE pathway to ally lipid accumulation and oxidative stress in steatotic HepG2 cells. *Eur. J. Pharmacol.* 882, 173244. doi: 10.1016/j.ejphar.2020.173244
- Sheng, J., and Sun, Y. (2014). Antioxidant properties of different molecular weight polysaccharides from *Athyrium multidentatum* (Doll.) ching. *Carbohydr. Polym.* 108, 41–45. doi: 10.1016/J.CARBPOL.2014.03.011
- Smith, B. K., Marcinko, K., Desjardins, E. M., Lally, J. S., Ford, R. J., and Steinberg, G. R. (2016). Treatment of nonalcoholic fatty liver disease: Role of AMPK. *Am. J. Physiol. Endocrinol. Metab.* 311 (4), E730–E740. doi: 10.1152/ajpendo.00225.2016
- Song, Y., Zhu, M., Hao, H., Deng, J., Li, M., Sun, Y., et al. (2019). Structure characterization of a novel polysaccharide from Chinese wild fruits (*Passiflora foetida*) and its immune-enhancing activity. *Int. J. Biol. Macromol.* 136, 324–331. doi: 10.1016/J.IJBIOMAC.2019.06.090
- Tan, X., Sun, Z., Liu, Q., Ye, H., Zou, C., Ye, C., et al. (2018). Effects of dietary ginkgo biloba leaf extract on growth performance, plasma biochemical parameters, fish composition, immune responses, liver histology, and immune and apoptosis-related genes expression of hybrid grouper (*Epinephelus lanceolatus* ♂ × *epinephelus fuscoguttatus* ♀). *Fish. Shellfish Immunol.* 72, 399–409. doi: 10.1016/j.fsi.2017.10.022
- Tan, X., Sun, Z., and Ye, C. (2019). Dietary *Lycium barbarum* extract administration improved growth, meat quality and lipid metabolism in hybrid grouper (*Epinephelus lanceolatus* ♂ × *E. fuscoguttatus* ♀) fed high lipid diets. *Aquaculture* 504, 190–198. doi: 10.1016/J.AQUACULTURE.2019.01.044
- Tao, W., Sun, W., Liu, L., Wang, G., Xiao, Z., Pei, X., et al. (2019). Chitosan oligosaccharide attenuates nonalcoholic fatty liver disease induced by high fat diet through reducing lipid accumulation, inflammation and oxidative stress in C57BL/6 mice. *Mar. Drugs* 17 (11), 645. doi: 10.3390/MD17110645
- Wang, K., Cao, P., Wang, H., Tang, Z., Wang, N., Wang, J., et al. (2016). Chronic administration of *Angelica sinensis* polysaccharide effectively improves fatty liver and glucose homeostasis in high-fat diet-fed mice. *Sci. Rep.* 6, 26229. doi: 10.1038/SREP26229
- Wu, Z., Li, H., Luo, Y., Chen, G., Li, J., Wang, Y., et al. (2020). Insights into the structural characterisations, bioactivities and their correlations with water-soluble polysaccharides extracted from different pomelo (*Citrus maxima merr.*) tissues. *Int. J. Food Sci. Technol.* 55, 3091–3103. doi: 10.1111/IJFS.14573
- Xiao, J., Guo, R., Fung, M. L., Liong, E. C., Chang, R. C. C., Ching, Y. P., et al. (2013). Garlic-derived S-allylmercaptocysteine ameliorates nonalcoholic fatty liver disease in a rat model through inhibition of apoptosis and enhancing autophagy. *Evid. Based. Complement Alternat. Med.* 2013, 642920. doi: 10.1155/2013/642920
- Yu, K., Huang, K., Jiang, S., Tang, X., Huang, X., Sun, L., et al. (2021). Protective function on liver and proteomic analysis of the improvement mechanism of *Sedum sarmentosum bunge* extract on nonalcoholic fatty liver disease in Nile tilapia. *Aquaculture* 531, 735977. doi: 10.1016/j.aquaculture.2020.735977
- Yu, Z., Zhao, L., Zhao, J. L., Xu, W., Guo, Z., Zhang, A. Z., et al. (2022). Dietary *Taraxacum mongolicum* polysaccharide ameliorates the growth, immune response, and antioxidant status in association with NF-κB, Nrf2 and TOR in jian carp (*Cyprinus carpio* var. jian). *Aquaculture* 547, 737522. doi: 10.1016/j.aquaculture.2021.737522
- Zang, L., Shimada, Y., Kawajiri, J., Tanaka, T., and Nishimura, N. (2014). Effects of yuzu (*Citrus junos siebold ex tanaka*) peel on the diet-induced obesity in a zebrafish model. *J. Funct. Foods* 10, 499–510. doi: 10.1016/j.jff.2014.08.002
- Zhang, Y., Chen, P., Liang, X. F., Han, J., Wu, X. F., Yang, Y. H., et al. (2019b). Metabolic disorder induces fatty liver in Japanese seabass, *Lateolabrax japonicus* fed a full plant protein diet and regulated by cAMP-JNK/NF-κB-caspase signal pathway. *Fish. Shellfish Immunol.* 90, 223–234. doi: 10.1016/j.fsi.2019.04.060
- Zhang, R., Jiang, Y., Zhou, L., Chen, Y., Wen, C., Liu, W., et al. (2019a). Effects of dietary yeast extract supplementation on growth, body composition, non-specific immunity, and antioxidant status of Chinese mitten crab (*Eriocheir sinensis*). *Fish. Shellfish Immunol.* 86, 1019–1025. doi: 10.1016/J.FSI.2018.12.052
- Zhang, X., Qi, C., Guo, Y., Zhou, W., and Zhang, Y. (2016). Toll-like receptor 4-related immunostimulatory polysaccharides: Primary structure, activity relationships, and possible interaction models. *Carbohydr. Polym.* 149, 186–206. doi: 10.1016/J.CARBPOL.2016.04.097
- Zou, C., Du, L., Wu, J., Gan, S., Li, Q., Sarath Babu, V., et al. (2022). Saikosaponin d alleviates high-fat-diet induced hepatic steatosis in hybrid grouper (*Epinephelus lanceolatus* ♂ × *epinephelus fuscoguttatus* ♀) by targeting AMPK/PPARα pathway. *Aquaculture* 553, 738088. doi: 10.1016/j.aquaculture.2022.738088
- Zou, C., Fang, Y., Lin, N., and Liu, H. (2021). Polysaccharide extract from pomelo fruitlet ameliorates diet-induced nonalcoholic fatty liver disease in hybrid grouper (*Epinephelus lanceolatus* ♂ × *epinephelus fuscoguttatus* ♀). *Fish. Shellfish Immunol.* 119, 114–127. doi: 10.1016/j.fsi.2021.09.034
- Zou, C., Su, N., Wu, J., Xu, M., Sun, Z., Liu, Q., et al. (2019). Dietary radix bupleuri extracts improves hepatic lipid accumulation and immune response of hybrid grouper (*Epinephelus lanceolatus* ♂ × *epinephelus fuscoguttatus* ♀). *Fish. Shellfish Immunol.* 88, 496–507. doi: 10.1016/j.fsi.2019.02.052
- Zou, C., Tan, X., Ye, H., Sun, Z., Chen, S., Liu, Q., et al. (2018). The hepatoprotective effects of radix bupleuri extracts against D-galactosamine/lipopolysaccharide induced liver injury in hybrid grouper (*Epinephelus lanceolatus* ♂ × *epinephelus fuscoguttatus* ♀). *Fish. Shellfish Immunol.* 83, 8–17. doi: 10.1016/j.fsi.2018.08.047